

文章编号: 2095-4980(2015)04-0653-06

# An intra-cavity absorption fiber gas sensor based on performance enhanced techniques

LI Mo<sup>1,2</sup>, YANG Fan<sup>1,3</sup>, LUO Yanhua<sup>2</sup>, PENG Gangding<sup>2</sup>

(1.Institute of Electronic Engineering, China Academy of Engineering Physics, Mianyang Sichuan 621999, China; 2.School of Electrical Engineering and Telecommunications, University of New South Wales, Sydney, 2052, NSW, Australia; 3.Information and Communication Company of Sichuan Electric Power Corporation, Chengdu Sichuan 610041, China)

**Abstract:** The performance of an erbium-doped fiber ring laser based intra-cavity absorption gas sensor was evaluated with performance enhanced techniques. A multi-line wavelength sweep technique and a weighted averaging technique were proposed for better gas detection. By selecting appropriate system parameters, 6 strong absorption lines near 1 530 nm of C<sub>2</sub>H<sub>2</sub> were obtained with good spectrum resolution in one scanning period. One group with higher absorption coefficients was used for relatively low gas concentration detection and the other with lower absorption coefficients was used for relatively high gas concentration. Both the groups can be used for medium gas concentration detection. For various concentration cases, by choosing proper absorption lines and performing weighted averaging, detection accuracy can be obtained over an extended detection range. The minimum detection limit could be very low after optimization.

**Key words:** fiber gas sensor; intra-cavity absorption spectroscopy; multi-line wavelength sweep technique; weighted averaging technique

**CLC number:** TN25

**Document code:** A

**doi:** 10.11805/TKYDA201504.0653

In the past twenty years, optical fiber gas sensors based on absorption of light within the range of 1 300 nm–1 800 nm have attracted great research interests. Numerous mechanisms were demonstrated with desirable features, such as high Signal-to-Noise Ratio(SNR), high sensitivity, fast response, compact size, immunity to electromagnetic interference and etc<sup>[1-10]</sup>. With these advantages, fiber gas sensors have been successfully used for detecting methane(CH<sub>4</sub>), acetylene(C<sub>2</sub>H<sub>2</sub>) and ammonia(NH<sub>3</sub>) in plenty of applications.

To get high detection sensitivity, one of the appropriate schemes is the Intra-Cavity Absorption spectroscopy Gas Sensor(ICAGS). It offers a simple and robust setup, formed by placing a gas cell into the laser cavity. The greatest advantage of ICAGS is, the laser beam transmits through the gas cell thousands of times, which effectively increases the absorption length with compact configuration and enhances the detection sensitivity. Hence even for trace gas, the sensitivity and detection limit are satisfactory.

By now, researchers have done lots of work about analyzing and enhancing the sensitivity and other performances of the ICAGS. In 2004, Y ZHANG et al reported an optical fiber gas sensor based on Erbium Doped Fiber(EDF) with 90 times enhanced sensitivity<sup>[11]</sup>. In 2008, K LIU et al proposed an ICAGS using wavelength sweep technique and wavelength modulation technique, with an improved detection limit of 75 ppm<sup>[12]</sup>. M LI et al analyzed the effects of the pump power, cavity loss, EDF dopant concentration and EDF length on the performance of the ICAGS and provided several selecting methods of system parameters<sup>[13-14]</sup>. Other researches also conducted work which helps for investigating, designing and optimizing an ICAGS for different usages<sup>[15-16]</sup>. For the above work, the sensitivity was greatly enhanced, while the experiments were always conducted in a narrow concentration range. One existing problem is how to get stable, precise results with high sensitivity in a wide range. In this paper, we will introduce our work on ICAGS with performance enhanced techniques for accurate gas detection results in an extended concentration range.

## 1 System configuration

The experimental ICAGS had a hardware part and a software part as shown in Fig.1. The hardware part contained an

Erbium Doped Fiber Amplifier(EDFA), an optical isolator, a variable attenuator, a Fabry-Perot Tunable Filter(F-P TF), a 50:50 optical coupler, a FBG and the electronic components. The EDFA was used to produce gain for a lasing operation, the isolator was applied to ensure one-direction operation and avoid hole burning, the variable attenuator was used to adjust the output power. By varying the driving voltage on the TF, the operating wavelength of the ICAGS was selected and the absorption spectrum of  $C_2H_2$  could be scanned. Because there existed a nonlinearity of the F-P TF, a compensation method was applied. The output was proportional to the gas concentration which was detected by a Photo Detector(PD) and then transformed into an electrical signal. The electrical signal was amplified by the pre-processing circuit and collected by a DAQ card. The DAQ card was also applied to provide an analogue driving signal to control the tuning voltage on the F-P TF. By applying I/O synchronization techniques in the LabVIEW program that was controlling the DAQ, one-to-one correspondence between the transmission wavelength and the detected absorption signal can be realized.

In the ICAGS, the gas cell is the place allowing for the gas absorption of the light. A pair of pig-tailed Gradient-index(GRIN) lenses and a steel tube with two openings on the side were used to form the gas cell in our ICAGS. Two GRIN lenses were fixed on a 4-axis adjustable platform with the gas cell between them. By adjusting the platform, the coupling losses of the GRIN lenses could be minimized. The loss of the gas cell was tested to be less than 10 dB with a length of about 10 cm. There were two narrow openings on the steel tube so that the gas can diffuse inside and outside.

## 2 Experimental results and analyses

Based on the system configuration shown in Fig.1, the gas detection was conducted. The software program generated a saw-tooth driving signal which was amplified to tune the F-P TF and to scan over the operation wavelength range of the ICAGS. The gas absorption lines of interest were recorded over each scan. The output power of the ICAGS corresponding to varying driving voltage was collected by the PD in this process. The driving voltage-output power relationship was translated as the wavelength-output power relationship. Therefore the wavelength, the shape and the amplitude of the absorption lines were obtained. Because the light intensity of the absorption lines is proportional to the gas concentration, by comparing the differences of the signal attenuations, the gas concentration can be calculated.

Here we proposed an improved multi-line wavelength sweep technique. The driving voltage of the TF was varied from 8.8 V to 9.75 V with a scanning step equal to 0.0017 V. One scan period was about 40 s across the absorption lines. In that voltage range, the absorption spectrum of 21.2%  $C_2H_2$  and spectrum with no  $C_2H_2$  at room temperature and one atmospheric pressure are shown in Fig.2. When the concentration of  $C_2H_2$  was 21.2%, 6 absorption lines were observed in one scan, the values of each absorption line varies due to the absorption of  $C_2H_2$ . The variation of each line is different because of different absorption coefficient (see Table.1). When there was no  $C_2H_2$ , no absorption happened in the gas cell.

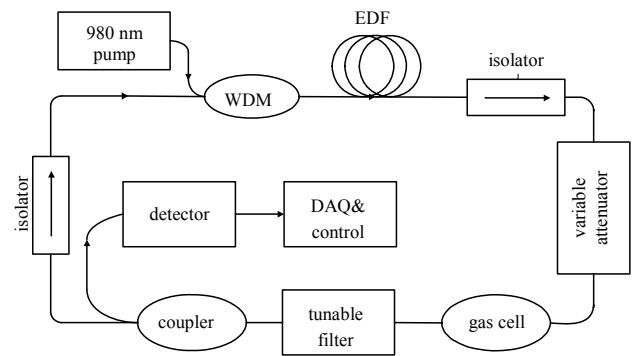


Fig.1 Configuration of the EDF based ICAGS

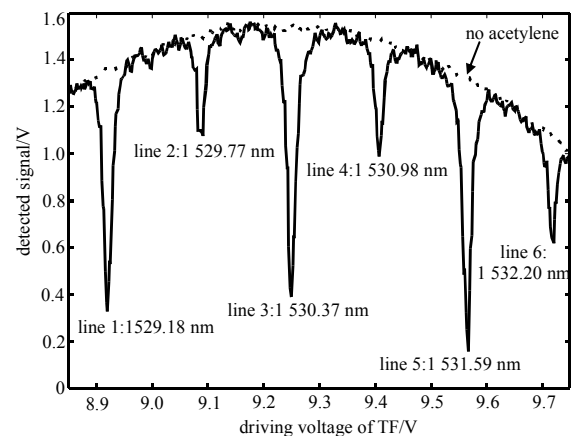


Fig.2 Absorption spectra of 21.2%  $C_2H_2$  and no  $C_2H_2$  in the gas cell with the driving voltage of F-P TF varying from 8.8 V to 9.75 V

At room temperature and one atmospheric pressure, the shape of the absorption line can be assumed as a Lorentzian profile. The collected data of the ICAGS were discrete points and required further signal processing. A series of experimental points near one single detected absorption line were selected and processed by Lorentzian curve fitting. The position of the fitted Lorentzian profile peak was used as the absorption central wavelength and its value was taken as  $I$  ( $I$  and  $I_0$  are the signal powers with and without gas absorption according to Lambert-Beer's law). Then several background signals of the two arms of the absorption profile were selected and fitted by a polynomial profile. By calculating the value of the fitted polynomial function at the central wavelength of the fitted Lorentzian profile,  $I_0$  can be obtained. The data processing procedure and the parameters of the absorption line of 42.2% C<sub>2</sub>H<sub>2</sub> are shown in Fig.3.

Table1 Absorption lines and absorption coefficients near 1530 nm

absorption line	central wavelength/nm	absorption coefficient/(cm <sup>-1</sup> /(molecule·cm <sup>-3</sup> ))
line 1	1 529.18	1.144 × 10 <sup>-20</sup>
line 2	1 529.77	3.977 × 10 <sup>-21</sup>
line 3	1 530.37	1.211 × 10 <sup>-20</sup>
line 4	1 530.98	4.002 × 10 <sup>-21</sup>
line 5	1 531.59	1.165 × 10 <sup>-20</sup>
line 6	1 532.20	3.693 × 10 <sup>-21</sup>

When the C<sub>2</sub>H<sub>2</sub> concentration is 92.6% and 5.5%, respectively, the absorption spectra are shown in Fig.4. We can see when the gas concentration was 92.6%, Line 1, Line 3 and Line 5 were saturated due to their high absorption coefficients. In this case, it was better to choose the signals of Line 2, Line 4 and Line 6 which were more precise. When the gas concentration was 5.5%, the signals of Line 2, Line 4 and Line 6 were very weak and had greater fluctuations which made them not suitable for use. However, the signals of Line 1, Line 3 and Line 5 were still strong. Therefore, we say for a relatively high gas concentration, Line 2, Line 4 and Line 6 have higher priority because they are not easy to saturate. While for a relatively low gas concentration, Line 1, Line 3 and Line 5 are better because they have stronger signal attenuation compared with that of the other 3 lines. When the gas concentration is medium, all the 6 lines can be used.

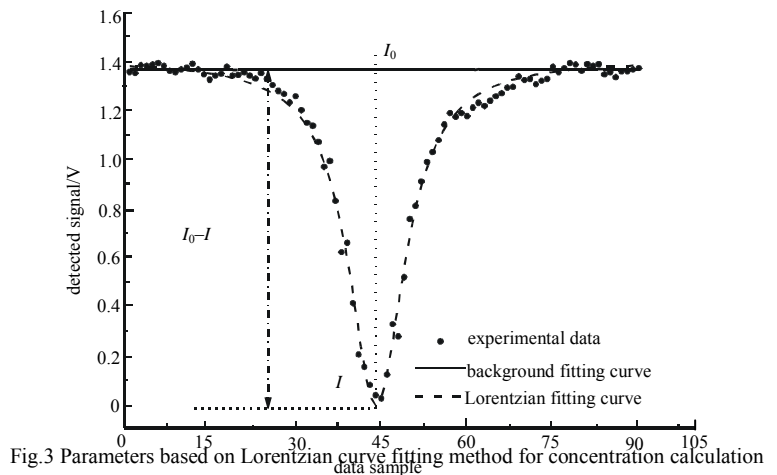


Fig.3 Parameters based on Lorentzian curve fitting method for concentration calculation

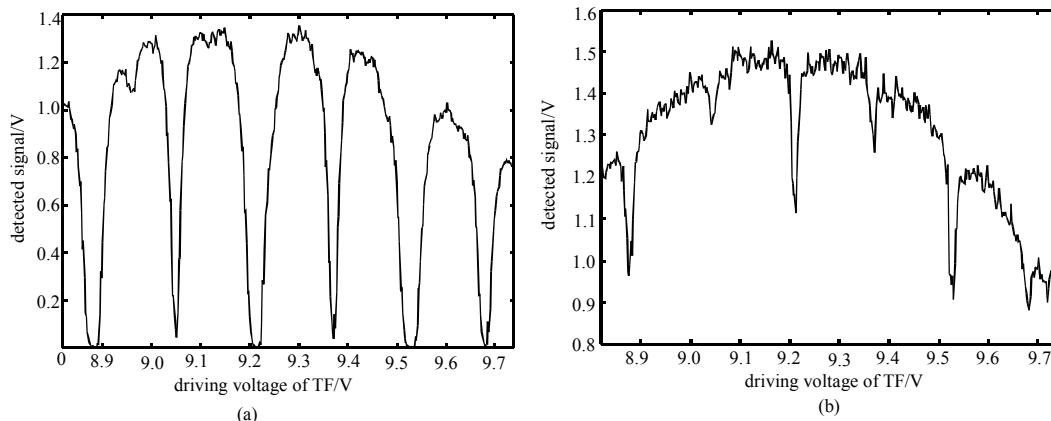


Fig.4 Absorption spectra of (a) 92.6% and (b) 5.5% C<sub>2</sub>H<sub>2</sub>

The gas absorption attenuation is assumed as  $10 \lg \left( \frac{I_0 - I}{I_0} \right)$  and the results of Line 1, Line 3 and Line 5 are shown in Fig.5 (a)<sup>[7]</sup>. When the C<sub>2</sub>H<sub>2</sub> concentration is lower than 13%, the relationship between the gas concentration and the

absorption attenuation exhibits good linearity and the linear curve fitting parameters are given in Table 2. With the gas concentration higher than 13%, the relationship between the gas concentration and the absorption attenuation are not linear. That is caused by the absorption saturation. When the gas concentration is high while the pump power is not enough strong, the intra-cavity gain cannot compensate the total loss including the loss induced by absorption and the inherit cavity loss fully. To increase the saturated concentration, the pump power can be set to a higher value to get enough gain.

The relationships between the signal absorption attenuation and the  $C_2H_2$  concentration of Line 2, Line 4 and Line 6 are shown in Fig.5 (b). With the concentration varying from 7.6% to 36%, this relationship exhibits good linearity and the linear fitting parameters are given in Table 3. With the concentration higher than 40%, however, the relationship between the gas concentration and the absorption attenuation are not linear any longer due to the saturated absorption. For a higher saturated threshold, the pump power should be increased and the cavity loss should be made lower. Basically, the saturated concentrations of Line 1, Line 3 and Line 5 are lower than those of Line 2, Line 4 and Line 6 because of the relatively high absorption coefficients of the former 3 lines.

Based on the multi-line wavelength sweep technique, absorption lines with higher absorption coefficient can be used for low concentration detection and lines with lower absorption coefficients can be used for high concentration detection. Hence, the absorption saturation can be avoided to a certain extent and the results are more reliable. The detection range is extended as well compared with that using only one absorption line.

	slope/(dB/percent)	intercept	general deviation/dB
line 1	31.29	-1.00	0.046 4
line 3	30.17	-0.91	0.045 3
line 5	39.36	-1.27	0.057 8

	slope percent/dB	intercept	general deviation/dB
line 2	8.860 0	-0.259 0	0.060 0
line 4	10.130 0	-0.360 0	0.079 6
line 6	14.150 0	-0.495 0	0.093 8

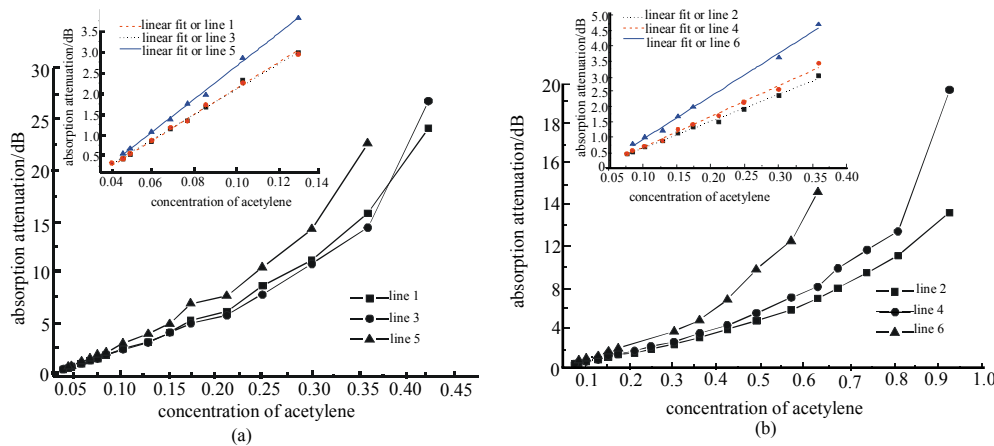


Fig.5 Absorption attenuation versus  $C_2H_2$  concentration

Moreover, different from a single-pass absorption gas sensor, the relationship between the signal attenuation induced by absorption versus gas concentration is not linear all the time. The pump power, cavity loss and other ICAGS parameters all affect this relationship. Lines with higher absorption coefficients saturate at lower  $C_2H_2$  concentrations. One of the simplest and most effective methods to reduce the effects of the saturation is to increase the pump power or decrease the cavity loss of the ICAGS.

To calculate the gas concentration of  $C_2H_2$ , instead of normally averaging the calculated results of 6 absorption lines, a weighted averaging method was designed. That is, in a certain concentration range, the absorption lines with lower relative errors or absolute errors have greater averaging weight and vice versa. The case when Line 3 and Line 4 are selected for calculation is taken as an example, we set the weighted averaging function of the two lines to calculate the  $C_2H_2$  concentration as below:

$$C_{\text{avg}} = \frac{M_3 C_3 + M_4 C_4}{M_3 + M_4} \quad (1)$$

$$\begin{cases} M_3 = 1, M_4 = 0, & (c < 22\%) \\ M_3 = 0, M_4 = 1, & (c \geq 22\%) \end{cases} \quad (2)$$

It always chooses the line with relatively lower errors. For this case, when the gas concentration is lower than 22%, the concentration of Line 3 with relatively lower relative and absolute errors is chosen; when the concentration is above 22%, the concentration of Line 4 is chosen which has

relatively lower errors in this range. The general deviations of the calculated and real concentrations using single Line 3, single Line 4, normal averaging method and weighted averaging method are listed in Table 4. We can see by applying the weighted averaging method, the calculation accuracy can be improved effectively. In particular, with proper weighted averaging factors the detection limit can be lower than 1 500 ppm.

	line 3	line 4	normal averaging	weighted averaging
general deviation	0.031 6	0.017 9	0.018 1	0.015 7
mean squared error	0.021 9	0.005 6	0.007 2	0.005 4

Therefore, based on the improved multi-line wavelength sweep technique, if 6 absorption lines with good resolution in one scan are applied, the detectable concentration range can be further extended. With a weighted averaging method, the detection accuracy can be improved over that using a single line or a normal averaging method. To further enhance the performance of the ICAGS, higher pump power or lower cavity loss can be introduced.

### 3 Conclusions

In this paper, the performance of the ICAGS in gas sensing was experimentally evaluated. The curve fitting method for absorption lines recognition and the calculation of the absorption signal were proposed. An improved multi-line wavelength sweep technique was applied in the ICAGS and 6 absorption lines obtained in one scan were divided into two groups. According to their absorption coefficients, the ones with higher absorption coefficients were suitable for relatively low concentration usage and the ones with lower absorption coefficients were suitable for relatively high concentration usage. Based on the relative and absolute errors at different  $C_2H_2$  concentration, a weighted averaging method of these lines was proposed with improved detection accuracy. This method also extends the concentration detection range of the ICAGS compared with conventional gas sensors. The minimum detection limit was lower than 1 500 ppm.

### References:

- [ 1 ] Dakin J P, Wade C A, Pinchbeck D, et al. A novel optical fiber methane sensor[C]// Proc. SPIE. London:[s.n.], 1997:187–190.
- [ 2 ] Uehara K, Tai H. Remote detection of methane using a 1.66  $\mu\text{m}$  diode laser in combination with optical fiber[C]// Proc. OFS7., 1990:51–54.
- [ 3 ] JIN W, Stewart G, Culshaw B. Source-noise limitation of fiber optic methane sensors[J]. Appl. Optics, 1995,34(13):2345–2349.
- [ 4 ] HO H L, WEI J, Demokan M S, et al. Multipoint gas detection using TDM and wavelength modulation spectroscopy[J]. Electronics Letters, 2000,36(14):1191–1193.
- [ 5 ] Sigrist M W. Trace gas monitoring by laser photoacoustic spectroscopy and related techniques[J]. Rev. Sci. Instrum, 2003 (74):486–490.
- [ 6 ] LI J S, GAO X M, LI F, et al. Resonant photoacoustic detection of trace gas with DFB diode laser[J]. Opt. Laser Technol., 2007(39):1144–1149.
- [ 7 ] Baev V M, Eschner J, Paeth E, et al. Intra-cavity spectroscopy with diode lasers[J]. Appl. Phys. B. 1992(55):463–477.
- [ 8 ] ZHANG M, ZHANG Y, WANG D N, et al. Fiber ring laser intra-cavity absorption spectroscopy for gas sensing[J]. Int. J. Nonlinear. Sci., 2002(3):569–572.
- [ 9 ] Wheeler M D, Newman S M, Orr-Ewing A J, et al. Cavity ring-down spectroscopy[J]. J. Chem. Soc. Faraday. Trans., 1998(94):337–351.
- [ 10 ] Stewart G, Shields P, Culshaw B. Development of fibre laser systems for ring-down and intracavity gas spectroscopy in the near-IR[J]. Meas. Sci. Technol., 2004(15):1621–1628

- [11] ZHANG Y,ZHANG M,JIN W,et al. Investigation of erbium-doped fiber laser intra-cavity absorption sensor for gas detection[J]. Optics Commun, 2004(232):295-301.
- [12] LIU K,JING W C,HO H L,et al, Wavelength sweep of intracavity fiber laser for low concentration gas detection[J]. IEEE Photonic. Tech. L. 20, 2008(2):1515-1517.
- [13] LI M,DAI J M, LIU K,et al. Performance analysis and design optimization of intra-cavity absorption gas sensor based on fiber ring laser[J]. J. Lightwave. Technol, 2011(29):3748-3756.
- [14] LI M,LIU K, JING W C,et al. Fiber ring laser intra-cavity absorption spectroscopy for gas sensing:Analysis and experiment[J]. J. Opt. Soc. Korea, 2010(14):14-21.
- [15] ZHANG M,WANG D N,JIN W,et al. Wavelength modulation technique for intra-cavity absorption gas sensor[J]. IEEE T Instrum. Meas, 2004(53):136-139.
- [16] ZHANG Y,ZHANG M,Jin W. Sensitivity enhancement in erbium-doped fiber laser intra-cavity absorption sensor[J]. Sens. Actuators A, 2003(104):183-187.

### Biography:



**LI Mo**(1982-), female, born in Heilongjiang Province, doctor's degree, associate professor. Main research fields include photonics, photonic and electronic integration technology, integrated microsystem technology, etc. email:limomaria@caep.cn.

**PENG Gangding**(1959-), male, born in Changsha, Hunan Province, doctor's degree, professor. Main research fields include laser technology, special fiber technology, optoelectronic technology, etc.

**YANG Fan**(1982-), male, born in Mianyang City, Sichuan Province, doctor's degree, engineer. Main research fields include optoelectronic technology, etc.

**LUO Yanhua**(1980-), male, born in Nanchang, Jiangxi Province, doctor's degree, associate professor. Main research fields include optoelectronic technology, special fiber technology, etc.

(上接第 648 页)

### 作者简介:



**湛治强**(1990-), 男, 四川省资阳市人, 初级技工, 主要从事半导体器件工艺. email: zhanzhiqiangty@sina.com.

**彭丽萍**(1979-), 女, 河南省周口市人, 博士, 主要研究方向为新型多功能薄膜材料、光电器件。

**王雪敏**(1975-), 男, 四川省泸州市人, 博士, 副研究员, 研究方向为新型多功能材料、光电器件等。

**阎大伟**(1984-), 男, 河南省焦作市人, 博士, 主要研究方向为新型多功能薄膜材料、光电器件。

**熊政伟**(1984-), 男, 四川省巴中市人, 博士, 主要研究方向为新型材料的制备与性能。

**沈昌乐**(1981-), 男, 江西省高安市人, 博士, 主要研究方向为新型多功能材料、光电器件。

**罗跃川**(1985-), 男, 四川省绵阳市人, 硕士, 主要从事微器件加工。

**吴卫东**(1967-), 男, 武汉市人, 博士, 研究员, 主要研究方向为 ICF 薄膜科学及制备技术、纳米材料等领域。